Journal of Thermal Analysis and Calorimetry (2019) 138:2691–2702
https://doi.org/10.1007/s10973-019-08799-0

Thermal expansivity and degradation properties of PLA/HA and PLA/βTCP in vitro conditioned composites

J. M. Ferri[1] · D. Luca Motoc[2] · S. Ferrandiz Bou[1] · R. Balart[1]

Received: 2 December 2018 / Accepted: 4 September 2019 / Published online: 16 September 2019

Abstract
The objective of this study was to investigate the thermal expansivities and degradation properties for several in vitro conditioned biodegradable poly(lactic acid)/hydroxyapatite (PLA/HA) and poly(lactic acid)/β-tricalcium phosphate (PLA/βTCP) composites with different mass% of the particle reinforcements (i.e. 10, 20 and 30). The samples were prepared by extrusion followed by injection moulding and incubated in a customized simulated body fluid at 37 °C over 60, 90, 120, 150 and 180 days, respectively. Thermal expansion and degradation properties of in vitro conditioned samples, along with dynamic mechanical properties of unconditioned ones, were systematically investigated through coefficients of linear thermal expansion and thermal strain changes, decomposition temperatures, mass changes and per cent residues. The results indicated that PLA/βTCP composites performed better than PLA/HA composites, irrespective of their filler mass%, revealing high values of glass transition temperatures, around a mean value of 65 °C, both on dynamic mechanical analysis and on dilatation measurements but lower values on their degradation temperatures, such as 360 °C. The results suggest the feasibility of tailoring high-loaded osteoconductive fillers-reinforced PLA composites for various medical and engineering applications.

Keywords Poly(lactic acid) · Hydroxyapatite · β-Tricalcium phosphate · Expansion · Degradation

Introduction

Poly(lactic acids) (PLAs) are the most deployed biodegradable polymers in healing products, surgical implant devices, orthopaedic devices, bioresorbable scaffolds for tissue engineering, packaging, textile and environmental applications because of their versatility, good mechanical, thermal and optical properties as well as the easy of processability on conventional laboratory equipment [1–3]. The interest in PLA is confirmed by extensive research papers and reviews in relation to its fabrication, processing and deployment for other combinations [4–7]. Taking advantage of the individual properties of PLA and accounting that the addition of fillers may enhance the effective properties of the polymeric compounds, various combinations with micro-fillers (e.g. talc, hydroxyapatite, inorganic carbonates, kaolin, etc.) or nanofillers (e.g. carbon nanotubes, halloysite, silica, etc.) were produced.

Hydroxyapatite (HA) is of high interest being a popular biomaterial which finds use as a bone or teeth replacement and repair, hard tissue repair. Balancing between advantages such as biocompatibility, osteointegration and osteoconductive properties and disadvantages including difficulties in processing owing to fragility and brittleness, PLA/HA composites were produced with synergistic effects on their material properties [8–11]. One of the main challenges when producing PLA/HA composites was the poor adhesion between the constitutive due to hydrophilicity of HA reinforcements in combination with the hydrophobic polymer matrix. The issue was overcome by modification on HA surface with silane and silane derivatives or phosphate-based solutions to enhance the

✉ D. Luca Motoc
danaluca@unitbv.ro; danalucamotoc@gmail.com

[1] Department of Mechanical and Materials Engineering, Universitat Politècnica de València, Plaza Ferrandiz y Carbonell, s/n, Alcoy, Alicante, Spain

[2] Department of Automotive and Transport Engineering, Transilvania University of Brasov, Eroilor Av., 500036 Brasov, Romania

dispersion within the PLA matrix and hence the interfacial adhesion [12, 13].

Another variation that captured researchers' attention is the β-tricalcium phosphate (βTCP) that in combination with PLA was widely deployed in tissue engineering for regeneration due to their enhanced biocompatibility and biodegradability [3, 14, 15]. Despite its brittleness that confines clinical application to no-load-bearing repair and substitution, good mechanical, dynamic mechanical and thermal properties were reported especially in highly loaded (amounts up to 30 or 40 mass%) composites [16] making this filler an ideal material implant. Ferri et al. [17] reported values in the range of 1.7–2.5 GPa for the tensile modulus, 4.95–5 GPa for the elastic modulus in flexure and 2.3 GPa for the storage modulus in shear for the 30 mass% fillers.

Addressing the osteoconductive and degradation behaviour of PLA and its composites for medical applications, in vitro simulations are demanded by immersing them into a simulated body fluid. These simulations can be done in either a static or dynamic fluid and further assess the performances of the specimens at various degradation grades [15, 18–20]. Kang et al. [14] approached the in vitro degradation under flowing conditions as well as dynamic loadings of PLA/βTCP composites within 4 and 6 weeks and measured the changes in mass, porosity, molecular weight and compressive strength. Further, Masanori et al. [20] shown that extension of immersion time length lowers the mechanical properties due to dissolution of βTCP from the surface.

In relation to the production of PLA composites, since NatureWorks LLC is the main leader in the market for PLA technology and production, their biopolymers under trademark Ingeo^{TM} are suitable for extrusion, injection moulding, solvent casting, pultrusion or hot pressing [21, 22]. Among previously, the twin-screw method is highly preferred in PLA-based composites manufacturing since enabling performance increase in material properties [23]. Additionally, fibre high demands for additive technologies (i.e. 3D printing) enabled high-loaded PLA/HA composite filaments production [24]. For example, Corcione et al. [25] reported one-step solvent-free process for fabrication of PLA/HA with mass% of 5, 15, 30 and 50, respectively, with glass transition temperatures (T_g) decreasing from 56.45 °C to 52.59 °C as the filler content increases. Next, Siqueira et al. [26] investigated the morphology and thermal properties of low-loaded PLA/βTCP (1, 5 and 8 mass%) fibres obtained by electrospinning. Their results show enhanced degree of crystallinity in high filler content, small differences in the T_g and good thermal stability from thermogravimetric measurements. Fused deposition method (FDM) is another technique deployed for PLA composites production. In a paper of Drummer et al. [27] were investigated the processing conditions on the mechanical and thermal properties of PLA/βTCP composites fabricated based on a FDM technique. Their findings point to several processing parameters that influence the mechanical properties and crystallinity of the material, such as the nozzle temperature set at 225 °C.

The aim of this contribution is to study the in vitro degradation of neat PLA, PLA/HA and PLA/βTCP composites manufactured by extrusion followed by an injection moulding process and to assess their dynamic mechanical, thermal expansion and thermal stability properties accounting both different mass% filler content and degradation time. This systematically approach aims to bring future insights in the behaviour of in vitro degradation of neat PLA- and high-loaded PLA/HA and PLA/βTCP composites to help tailoring novel bioabsorbable materials for specific application and various recipients.

Experimental

Materials selection

The matrix deployed for herein research is a NatureWorks LLC (Minnetonka, USA) poly(lactic) (PLA) biopolymer, Ingeo^{TM} 6201D delivered as pellets. Both injection moulding and extrusion processes can be used owing to the intrinsic PLA material properties, such as melt flow index 15–30 g 10^{-1} min^{-1} (210 °C), density 1.24 g cm^{-3} and melting temperature of 150–170 °C. Further, the glass transition temperature varies between 55 and 60 °C.

The hydroxyapatite constitutive (HA)—$Ca_5(OH)(PO_4)_3$ (Sigma-Aldrich, DE), supplied as nanoparticles with mean size ≤ 200 nm, containing 35–40% Ca (Ca/P ratio is 1.67), and the β-tricalcium phosphate—$Ca_3(PO_4)_2$ (Sigma-Aldrich, DE), supplied as powder with average particle size of 4 μm ± 2 μm, are acting as reinforcements for the PLA polymer matrix.

PLA and PLA composites preparation and conditioning

The unfilled PLA and PLA-based composites were produced with different mass% as reported in the previous contributions [17, 28] and further labelled as PLA, PLA-xx% HA and PLA-xx% βTCP to differentiate among neat, HA or βTCP-reinforced composites of different mass fractions used (i.e. 10, 20 or 30). The PLA pellets were dried prior manufacturing at 80 °C for 24 h to remove residual moisture and reduce hydrolysis effects during their processing. PLA/HA and PLA/βTCP composites specimens' manufacturing was initiated by melt blending the

components into a L/D relation by a 24 twin-screw co-rotating extruder at 60 rot min^{-1}. The temperature profile exhibited the values of 170 °C, 175 °C, 177.5 °C and 180 °C from the hopper to the die. After cooling, the mixtures were further pelletized and processed by injection moulding on a Meteor 270/75 machine (Mateu and Sole, ES) at 180 °C. The samples were injected at a pressure of 1400 bar. The cycle time was 17 s, and the mould temperature reached 50 °C. Samples were delivered under plain rectangular shapes with the following dimensions: 80 × 10 × 4 mm^3, covering thus different potential testing requirements. In vitro studies were performed by immersion the sample in a in situ prepared phosphate-buffered solution (SBF) [29] accounted to simulate fluid body conditions, at a constant temperature of 37 °C. Fresh SBF was added into the chamber at every removing time length (30, 60, 90, 120, 150 and 180 days, respectively) keeping the immersion volume constant during the experiment.

Composite samples characterization

Dynamic mechanical analysis (DMA)

Dynamic mechanical measurements were taken by aid of a controlled stress rheometer AR-G2 (TA Instruments, New Castle, USA) at a frequency of 1 Hz, in torsion mode, within 25–110 °C temperature range, using a 2 °C min^{-1} heating rate in the dynamic step. The experimental runs comply the ASTM D5279-13 standard procedure. Plano-parallel sample dimensions were set as 40 × 10 × 4 mm^3 and were cut by aid of a diamond disc cutting machine. Measurement set up and data acquisition were handled in the Rheology Advantage Instrument Control AR environment enabling information gathering for the storage modulus in shear (G') and damping curves (tan δ).

Dilatometry (DIL)

Specimens' expansivity was monitored by aid of a push rod dilatometer DIL 402 PC (Netzsch GmbH, D), in controlled atmosphere, within 25–95 °C temperature range deploying 2.5 K min^{-1} heating rate in the dynamic step, followed by a 15 min isothermal. The experimental runs comply the ASTM E228:2011 standard procedures. Specimens' dimensions were set as 25 mm × 5 mm in length and width, respectively, shaped by aid of the same cutting device as previously. Accompanying software Proteus® enabled outcomes retrieval, such as the coefficient of linear thermal expansion (CLTE or α), technical alpha (α_T) inflexion points and their corresponding glass transition temperatures (T_g), namely.

Thermogravimetric analysis (TGA)

Thermogravimetric analysis on specimens was performed by aid of a STA 449 F3 Jupiter® (Netzsch GmbH, D) at a heating rate of 10 °C min^{-1}, in controlled N_2 atmosphere at a 20 mL min^{-1} flow rate. The measurements comply the ISO 11358-1:2014 procedures. Dynamic mode was deployed in the heating step within the selected 25–650 °C temperature range. Alumina crucible was used for each individual specimen excerpt. The mass loss was recorded in response to temperature increases.

Scanning electron microscopy (SEM)

Specimens morphology was investigated by aid of a field emission scanning microscope FESEM Zeiss Ultra55 (Oxford Instruments, UK) at an acceleration voltage of 2 kV. The samples were subjected to a cryofracture process by aid of liquid nitrogen. To enhance image details on the particle dispersion the samples were sputtered with platinum in a sputter coater EMITECH SC7620 (Quorum Technologies Ltd., UK). Along with the previous device, a scanning microscope (SEM) module Phenom (FEI Company, Eindhoven, NL) was deployed to characterize the samples surface morphology from a different perspective. In this case, the surfaces were sputtered by an Au–Pd alloy.

Results and discussion

Morphological characterization of PLA/HA and PLA/βTCP composites

Morphologies of PLA/HA and PLA/βTCP composites are shown in the excerpts in Figs. 1 and 2. As it can be seen

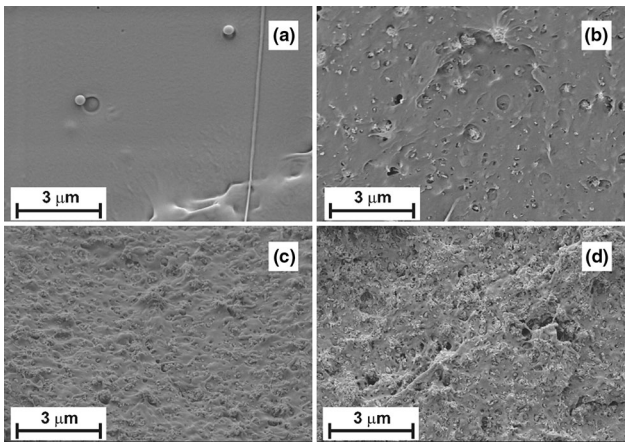

Fig. 1 FESEM images at ×10,000 on cryofractured surfaces of PLA/HA composites with different mass% hydroxyapatites: **a** neat PLA, **b** 10 mass% HA, **c** 20 mass% HA and **d** 30 mass% HA

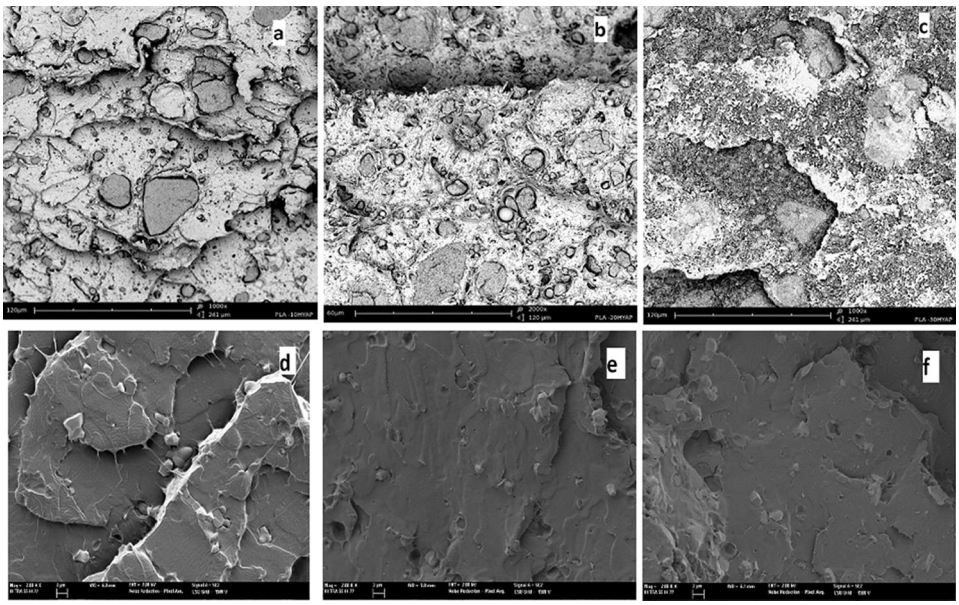

Fig. 2 SEM images of PLA composites with different mass% fillers: **a** 10 mass% HA, **b** 20 mass% HA, **c** 30 mass% HA, **d** 10 mass% βTCP, **e** 20 mass% βTCP and **f** 30 mass% βTCP

from the FESEM images on the PLA/HA composites (see Fig. 1), along with increase on the mass% content, the surfaces are becoming rougher and more porous and the fracture process can be characterized as fragile in its essence. Additionally, HA fillers have good dispersion within the PLA matrix with enhanced filler/matrix interface at lower mass% contents, as further seen in Fig. 2a–c. On the other hand, the FESEM images of PLA/βTCP (see Fig. 2d–f) reveal less particle dispersion within the PLA matrix compared with their HA counterparts. The particles of βTCP are more hydrophilic than the HA particles. As a result, βTCP particles aggregates degrade the mechanical properties of their compounds, behaving as crack initiators as already reported [17, 29].

Dynamic mechanical properties of PLA/HA and PLA/βTCP composites

Dynamic mechanical properties of neat PLA and PLA/HA or PLA/βTCP composites were retrieved within selected temperature range and oscillating frequency of 1 Hz to provide insights in the interfacial adhesion between HA or βTCP reinforcements and the PLA matrix in addition to SEM images.

Figure 3 shows the variation of storage modulus in shear (G') of PLA, PLA/βTCP and PLA/HA composites within temperature range. As can be seen, the G' of all samples preserves approximatively a constant evolution with temperature increase below their glass transition temperature T_g. Additionally, PLA/HA and PLA/βTCP composites exhibit higher values of G' compared with neat PLA and ascending with the increase in HA and βTCP mass fraction, thus samples becoming stiffer. Further, the slope of the

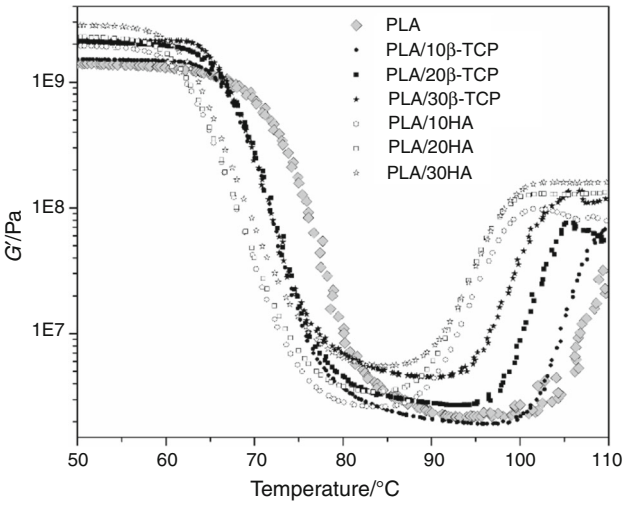

Fig. 3 Storage modulus (G') over temperature range of unconditioned PLA/HA and PLA/βTCP composites

glass transition T_g varies for PLA/HA composites, the abrupt decrease within a relatively narrow temperature range showing both an enhanced interfacial adhesion between the PLA matrix and HA reinforcements and the ability of former to withstand frequency depended mechanical loadings. However, no variation is observed in the T_g evolution in all PLA/βTCP composites due to the non-matrix-particle interaction. In the rubbery plateau, samples' behaviour follows an increased tendency. These variations can be ascribed to the cold crystallization transition occurring at temperatures above 95 °C. The higher the content of βTCP, the lower the temperature of crystallization process occurrence. This indicates that βTCP reinforcements act as a nucleating agent in the process.

In line with above, interface adhesion between PLA matrix and HA or βTCP fillers of different mass% can be further sized by exploring their corresponding damping curves (tan δ) as plotted in Fig. 4. Generally, lower tan δ values point towards good adhesion at matrix/filler interface due to reduction in the chain polymer mobility, whereas higher values suggest weak adhesion [30]. These curves are further deployed to recover glass transition temperatures T_g of the samples under discussion. The values are, as following: PLA—69.44 °C; PLA/HA composites—55.89 °C, 56.08 °C and 54.54 °C; PLA/βTCP composites—65.92 °C, 65.72 °C and 64.50 °C, respectively, in mass% increasing order. Supplementary, the decrease in T_g values is due to a variation in the degree of crystallinity. Ferri et al. [29] showed that the degree of crystallinity lowers as the HA content increases. Owing to HA particles' hydrophilicity, a hydrolysis process occurs during the specimen manufacturing due to the moisture within these particles. As a result, the lactic acid oligomers produced will plasticize the PLA matrix, enabling the polymer chains to move easier. Thus, as the HA content increases, the presence of moisture increases and larger chain cleavages occur, allowing greater mobility of the polymer chains. The slight shift in the T_g values for each materials class can be assigned to mass% filler content. The height of tan δ is associated with the mobility of amorphous region in the polymer matrix. As presented, PLA/βTCP composites exhibit sharp and high tan δ peaks indicating that they have good structural damping properties and consequently improved capacity to absorb mechanical energy compared to neat PLA. Comparatively, PLA/HA composites not only exhibit a reduction in the sharpness and height of their tan δ peaks but accentuated left shift of T_g values.

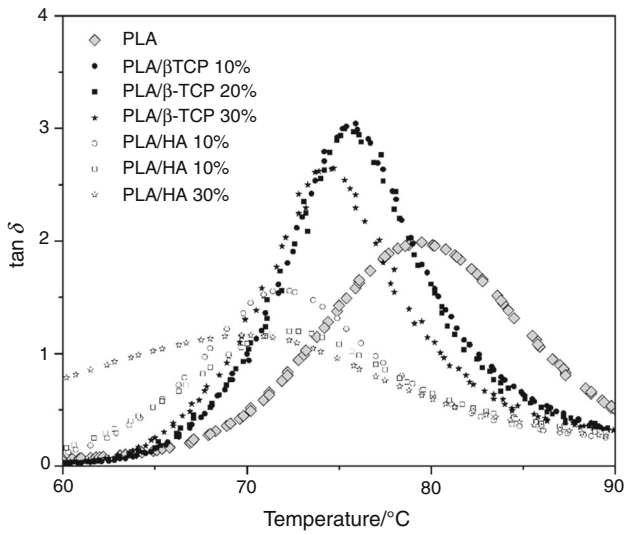

Fig. 4 Damping curves of unconditioned neat PLA, PLA/HA and PLA/βTCP composites

Thermal expansion of PLA/HA and PLA/βTCP composites

Dilatometry measurements aimed to bring supplementary information on the PLA and PLA composites behaviour with temperature from thermal expansivity perspective. Thus, along with the physical alpha K^{-1} (CLTE—coefficient of linear thermal expansion) and thermal strain fields developed within in vitro conditioned PLA and PLA composites under discussion, technical alpha (α_T, K^{-1}) was additionally provided since represents a unique value within an imposed temperature values (25–95 °C) to be used as further reference.

Further insights in this thermal property was considered by collecting the CLTE values at 37 °C that corresponds to an average temperature of human body following one of the major application domains of these PLA-based composites, namely bone fixtures. Table 1 lists these values for all specimens covering selected mass% of HA and βTCP fillers over the in vitro conditioning days. A closer look into the values, generally, reveals a decrease tendency with the increase mass% of the inorganic filler, both HA and βTCP fillers for identical time conditioning range as well as, individually, with degradation time increase.

Inorganic fillers significantly reduce thermal expansion values as their mass% increases, statement that can be easily prove if considering the simple rule of mixture during that the polymer matrix content reduces [31]. Another influencing factor can be regarded to the cooling time during the specimen preparation especially in semi-crystalline polymers whose crystallization process requires time. The latter was not investigated herein and thus was hypothetically accounted [25, 32].

The influence of in vitro conditioning upon expansivities of PLA and PLA-based composite specimens was further investigated, and it can be sized in the curves of Fig. 5 that represents excerpts from the database. The CLTE in all specimens exhibits the same tendency over temperature with minor discrepancies due to the different mass% of fillers. Additionally, there are differences among HA and βTCP-reinforced PLA composites, the latter revealing the lowest variation over the temperature range. One reason for this behaviour can be regarded to the random distribution of the HA and βTCP fillers within the PLA matrix and furthermore to the increases in the agglomeration degree as the mass% increases. Further, intakes during the immersion within simulated fluid body pose supplementary influence since it causes both mass changes and changes in porosity [14]. These can be sized better in the changes due to immersion times up to 90 days (3 months) followed small

Table 1 CLTE 10^{-5} K^{-1} of PLA, PLA-HA and PLA-βTCP in vitro conditioned samples, retrieved at temperature of 37 °C

Days	PLA	PLA-10%HA	PLA-20%HA	PLA-30%HA	PLA-10%βTCP	PLA-20%βTCP	PLA-30%βTCP
0	7.3008	6.9734	7.1013	6.2054	6.3177	6.7050	6.2941
30	7.2918	7.0929	7.0549	6.3621	6.1344	6.5369	6.4274
60	6.9816	6.8994	7.0348	6.5614	6.4546	6.6789	6.3347
90	7.2317	7.2546	7.2757	6.5256	6.7862	6.7476	6.2611
120	7.3728	7.3247	7.5189	6.9607	6.8317	6.7442	6.4398
150	6.7815	7.0931	6.6381	6.5462	6.4963	6.5001	6.1178
180	7.0029	7.3561	7.3238	7.288	6.549	6.4561	6.6908

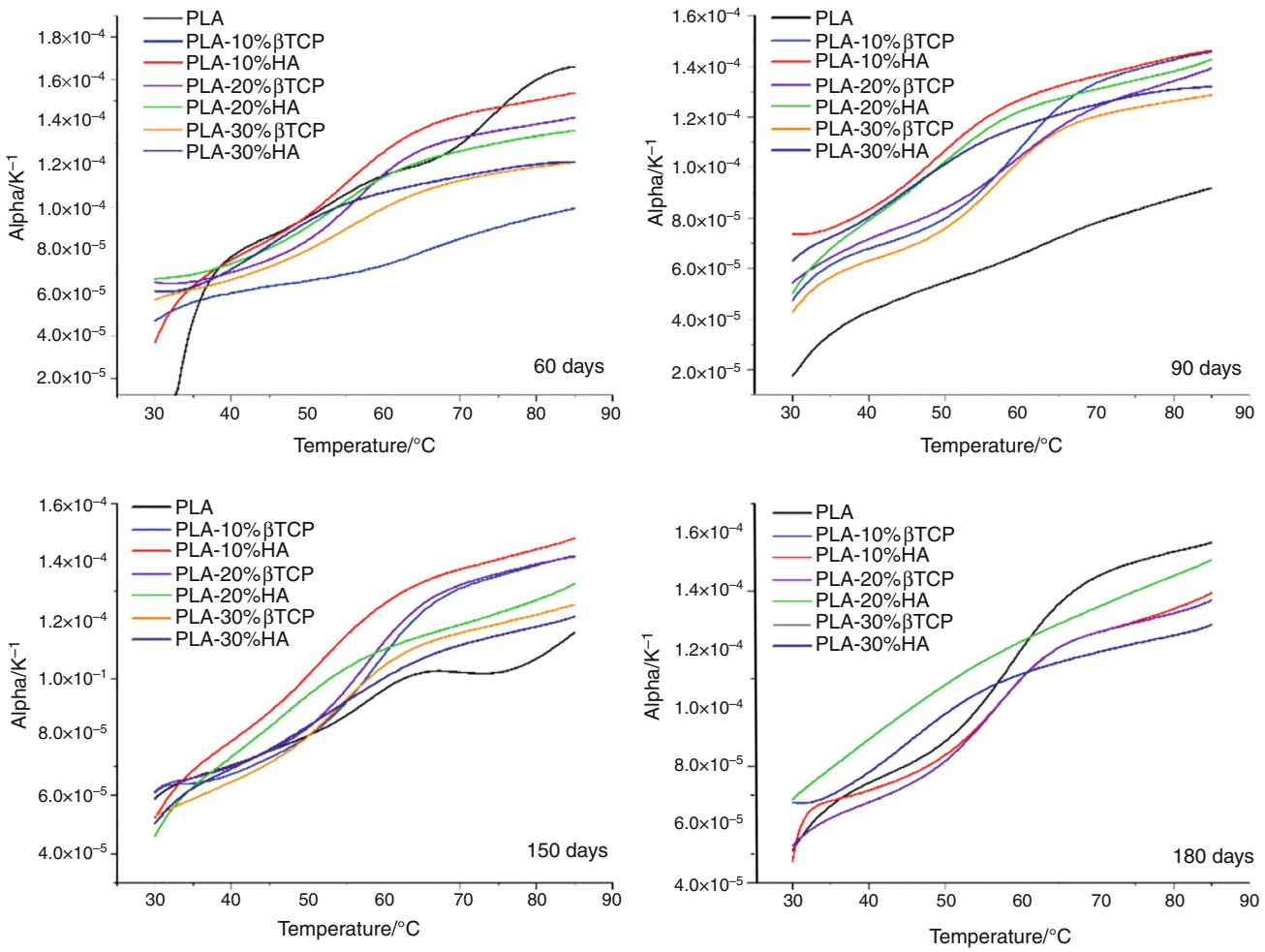

Fig. 5 Physical alpha over temperature range of in vitro conditioned neat PLA, PLA/HA and PLA/βTCP composites (60, 90, 150, 180 days)

variations caused by further exposure to the simulated body fluid for 150 and 180 days, respectively. This is consistent with the degradation rates of the scaffolds that should match the formation of a new bone that is being shifted with one month compared with the reported time intervals, due to the high HA and βTCP loading within the PLA matrix [15]. Further, the linear expansion is higher above 45 °C in neat PLA and PLA composites herein (above T_g as follows) as polymer chain mobility changes due to a crystallization process.

With respect to the thermal strain developed within the PLA, these revealed identical trends in all specimens irrespective of the inorganic fillers and mass% deployed, as it can be seen in the excerpt plots from Fig. 6. A closer

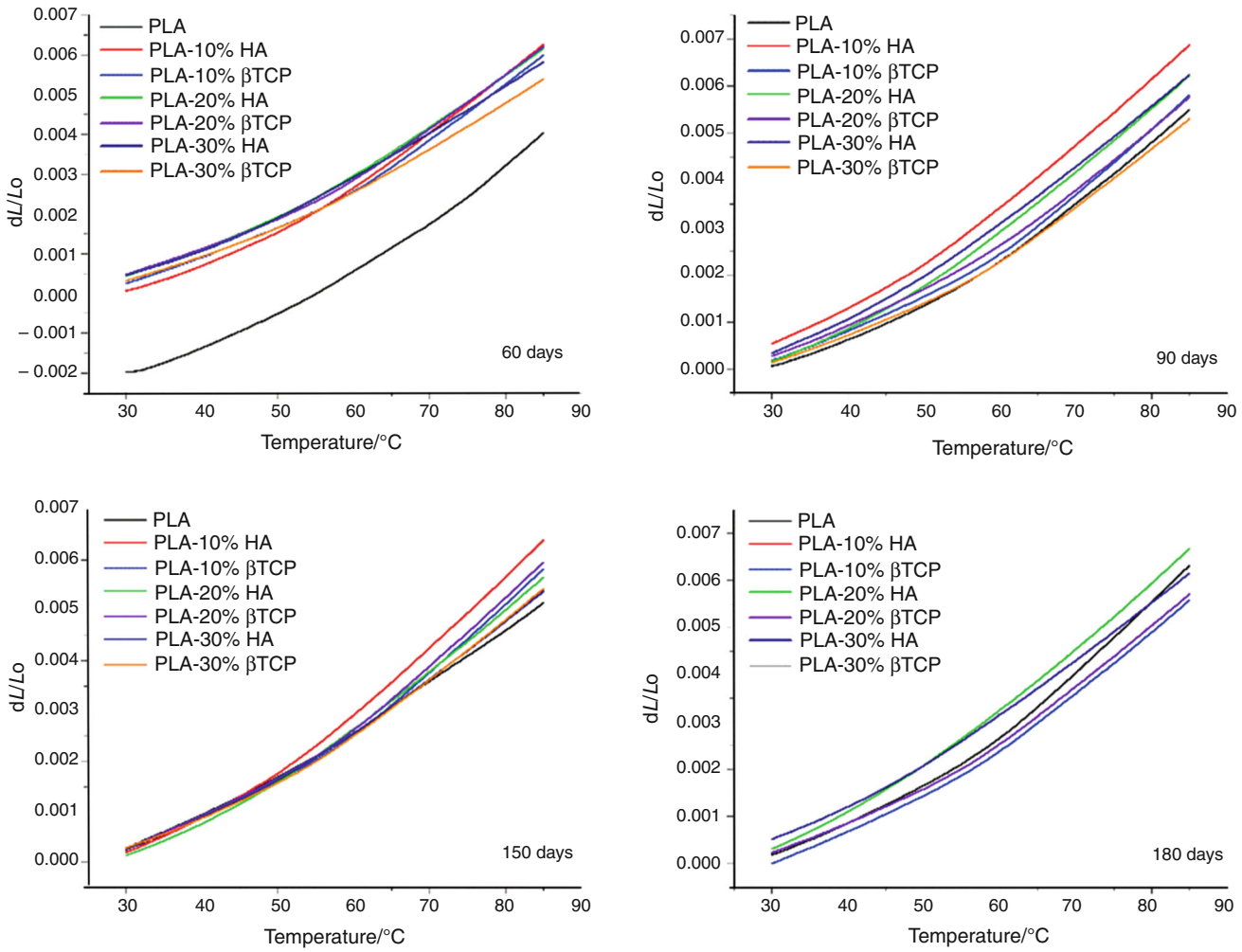

Fig. 6 Thermal strain over temperature range of in vitro conditioned neat PLA, PLA/HA and PLA/βTCP composites (60, 90, 150, 180 days)

Table 2 T_g/°C values of PLA, PLA-HA and PLA-βTCP in vitro conditioned samples from DIL measurements

Days	PLA	PLA-10%HA	PLA-20%HA	PLA-30%HA	PLA-10%βTCP	PLA-20%βTCP	PLA-30%βTCP
0	62.3	57.6	52.9	50.6	61	60.5	58.1
30	60	62.4	53.6	53.9	59.7	61.8	57.2
60	62.9	54.8	53.7	45.3	60	56.5	55.4
90	61.1	48.9	49.7	45.5	59.7	59.4	57.2
120	59.6	51.2	61.8	52.3	59.6	57.7	57.7
150	57.9	51.5	59.8	51.18	59	59	54.6
180	58.7	57.4	51.8	45.7	56.4	56.6	53.1

look reveals the influence of the immersion time especially upon the PLA specimen individually that is more pronounced in the 60-day conditioned sample, while the previous apply for debates on the measures.

Physical alpha curves enable glass transition temperature T_g retrieval, as provided in Table 2 for all specimens and immersion time lengths considered. A general decreasing tendency of T_g values in all PLA and PLA composites can be sized over the immersion time range, more pronounced in 30 mass% HA-reinforced PLA samples, from 53.9 °C to 45.3 °C and 45.7 °C, respectively. These are consistent with the previous findings from differential scanning calorimetry (DSC) measurements on unconditioned PLA/HA composites [28]. On the other

hand, for the PLA/βTCP in vitro conditioned samples, minor changes are encountered along with their mass% increase as well as with immersion time. This can be related to the good particle distribution within the PLA matrix. The values fluctuate around 59 °C with two exceptions. One holds in the highest immersion time (180 days) where the T_g values are decreasing around 56 °C in all samples and the other in the 30 mass% βTCP-reinforced PLA matrix. Further, as debated in the cited references of the previous works of the herein research group, this can be related to the partial hydrolysis of PLA polymer chain due to the highly loaded and hydrophilic HA and βTCP fillers that not only hydrolyze the ester groups of PLA matrix but promote a plasticization process with the formed lactic acid oligomers.

Another value of interest is technical alpha (α_T) that was computed over the temperature range against a reference temperature (25 °C in this case) to enable both a quick data analysis and reference values to other studies, database or computer simulations. Therefore, Fig. 7 shows the variation of this property for unfilled PLA, PLA/HA and PLA/βTCP composites over the immersion time. Generally, similar lowering effects hold with the addition of HA and βTCP fillers within the PLA matrix, as previously identified. Supplementary, the preceding debates are exposed as abrupt variations over time in the PLA/HA samples and small changes as those encountered in the PLA/βTCP composites. Again, measurements on samples immersed within 90 days reveal differences that can be regarded to the maximum simulated fluid body intakes and degradation, and further considered as initial points of the saturation process.

Thermal degradation of PLA/HA and PLA/βTCP composites

The thermogravimetric (TG) and derivative thermogravimetric (DTG) curves of PLA/βTCP excerpts corresponding to 10% and 30% filler loadings, respectively, immersed in simulated body fluid are shown in Figs. 8 and 9. All composite samples exhibit one main decomposition step under pyrolytic conditions, with onset temperatures within 300–333 °C range, while differences are due to different filler mass% content.

Insights in the degradation process can be accounted from the TG characteristic temperatures of unconditioned PLA, PLA/HA and PLA/βTCP composites at a heating rate of 10 K min^{-1} as provided in Table 3 and further from the decomposition temperatures (T_d) corresponding to 25%, 50% and 75% specimen mass loss as listed in Table 4 for the degraded samples. Since it is beyond of the purpose of this study to debate on degradation temperature and methods used to be identified (either maximum peak of DTG curve or temperature at 50% mass loss of the sample) to have an indication of destabilization as suggested in the literature, we will focus next on the values listed in above tables [13].

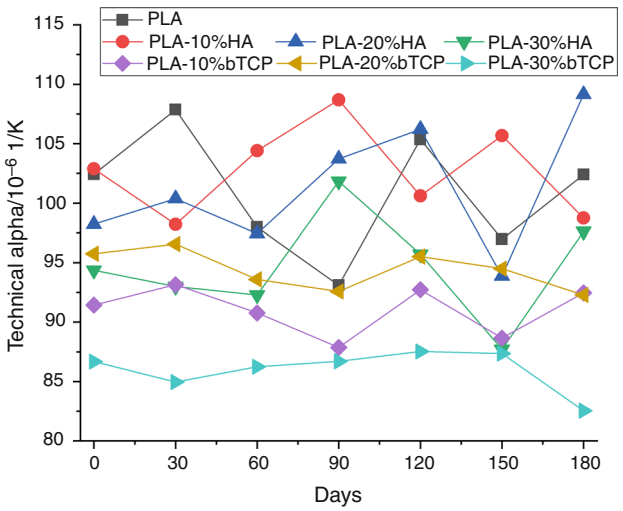

Fig. 7 Technical alpha variation with in vitro conditioning time of PLA, PLA/HA and PLA/βTCP composites

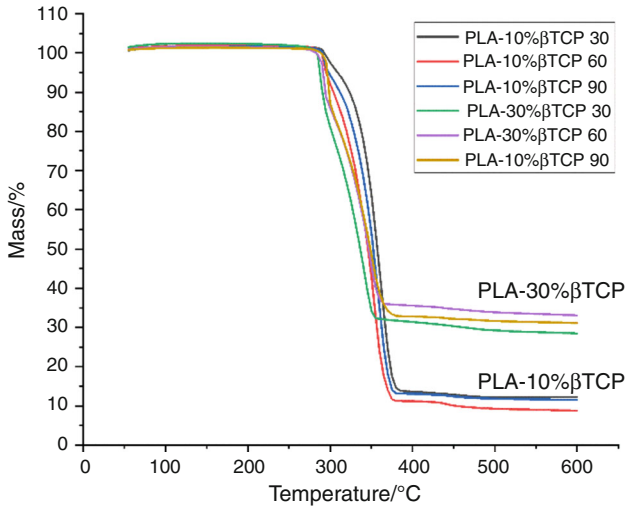

Fig. 8 Temperature-dependent mass change (TG) of in vitro conditioned 10 mass% and 30 mass% PLA/βTCP composites

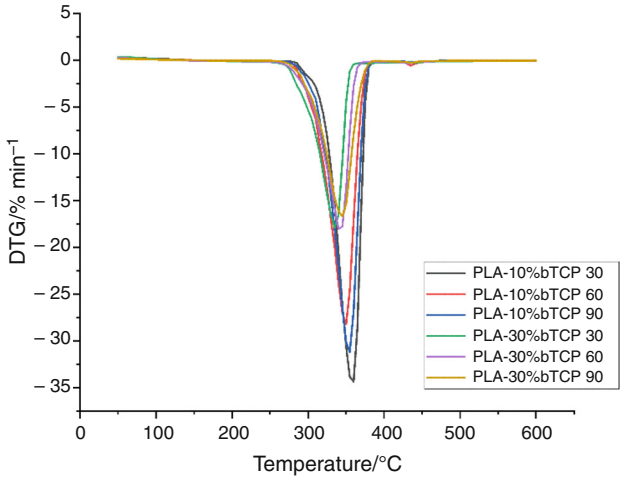

Fig. 9 Rate of mass change (DTG) of in vitro conditioned 10 mass% and 30 mass% PLA/βTCP composites

Thermal stability of PLAs was reported to be poor and highly sensitive to heat due to intramolecular trans-esterification resulting in the formation of lactide oligomers, carboxylic groups, etc. [3, 33]. In this study, the improved stability of in vitro conditioned samples can be explained by the manufacturing method that resulted in water removal. Supplementary, it is noteworthy to underline that highly loading the PLA matrix with HA or βTCP results in improvements of the thermal stability of all composite systems. HA-reinforced PLA composite systems revealed an increase in their onset degradation temperature with the addition of inorganic filler, from 326 °C up to 333 °C with fillers' mass% increase. Comparatively, βTCP-reinforced PLA composites show a decrease in the values from 305 °C to 297.7 °C of the same measure, with fillers' mass% increase. As for the decomposition temperatures associated with the maximum peak of DTG curves, high values are identified in PLA/HA composites compared with their counterparts, PLA/βTCP for all mass% considered, resulting in improvements on the thermal stability of the former composition.

In Table 3 were provided the percentage residues for neat PLA, PLA/HA and PLA/βTCP composites. These values increase with the increase of the mass% of the fillers, either HA or βTCP, the higher the amount the higher samples' thermal stability. In highly loaded PLA composites (20, 30 mass%), the residues are comparable: 19.5% for PLA-20%HA and 22.8% for PLA-20% βTCP, 28.95% for PLA-20%HA and 28.7% for PLA-20% βTCP, respectively, and include small quantities of residual ashes from PLA.

Following the contribution of Schindler et al. [34] and the known correlations between glass transition and melting temperatures [35] as well as between melting and decomposition temperatures, our experimental data were shaped as illustrated in Fig. 10. The values correspond to the unconditioned PLA, PLA/HA and PLA/βTCP samples aiming to ease data comparison accounting similar values from other contributions or to further tailor these combinations.

From Fig. 10, it can be concluded that PLA polymer has the highest glass transition and melting temperatures but relatively a low decomposition temperature. This behaviour does not preclude its identification by means of a dedicated software. Additionally, these plots outline better the differences debated due to filler type, either HA or βTCP. As it can be seen, the tendency points towards a clustering effect in all mass% considered. PLA/βTCP composites are characterized by high values of their glass temperatures but reduced decomposition temperatures, whereas PLA/HA composites reveal high values on their decomposition temperatures.

Table 3 Thermal degradation results of PLA, PLA/HA and PLA/βTCP samples

Mass loss data	PLA	PLA-10%HA	PLA-20%HA	PLA-30%HA	PLA-10%βTCP	PLA-20%βTCP	PLA-30%βTCP
T_{onset} (°C)	326.2	326.6	333.3	333.8	305.0	300.5	297.7
T_{mid} (°C)	357.7	369.9	375.4	378.5	357.3	361.8	359.4
T_{max} (°C)	364.6	370.5	377.3	378.9	360.9	364.0	359.1
T_{end} (°C)	377.6	392.2	399.7	396.8	374.9	374.2	369.8
Mass change%	96.71 (651 °C)	91.05 (650.3 °C)	80.5 (650.1 °C)	71.05 (650.7 °C)	87.9 (650.1 °C)	77.2 (650.2 °C)	71.3 (650 °C)
Residual mass%	3.29 (651 °C)	8.95 (650.3 °C)	19.5 (650.1 °C)	28.95 (650.7 °C)	12.1 (650.1 °C)	22.8 (650.2 °C)	28.7 (650 °C)

T_{onset}, initial temperature of the degradation curve; T_{mid}, temperature with the middle of degradation curve; T_{max}, temperature of highest degradation; T_{end}, final temperature of the degradation curve

Table 4 Decomposition temperatures for PLA, PLA/HA and PLA/βTCP samples for different mass loss values

Samples	T_d/°C											
	25%				50%				75%			
	30 days	60 days	90 days	180 days	30 days	60 days	90 days	180 days	30 days	60 days	90 days	180 days
PLA	356.1	349.5	354.3	354.7	366.1	358.1	364.3	364.5	375.3	366.0	373.3	373.6
PLA-10%HA	356.7	354.1	355.3	350.6	367.3	365.4	366.5	363.3	379.3	376.0	377.4	374.3
PLA-20%HA	357.1	356.3	355.3	346.9	368.6	368.4	366.4	362.6	382.9	381.5	377.3	377.2
PLA-10%HA	358.3	354.9	351.6	353.0	370.0	369.5	368.3	367.7	–	–	–	–
PLA-10%βTCP	352.9	350.6	347.4	346.8	355.7	353.8	350.4	349.1	358.1	355.5	353.1	351.1
PLA-20%βTCP	350.5	348.5	346.1	338.3	353.7	353.3	348.9	341.6	356.0	354.5	351.7	345.3
PLA-30%βTCP	345.1	343.9	341.3	330.1	348.5	347.8	339.8	335.7	–	–	–	–

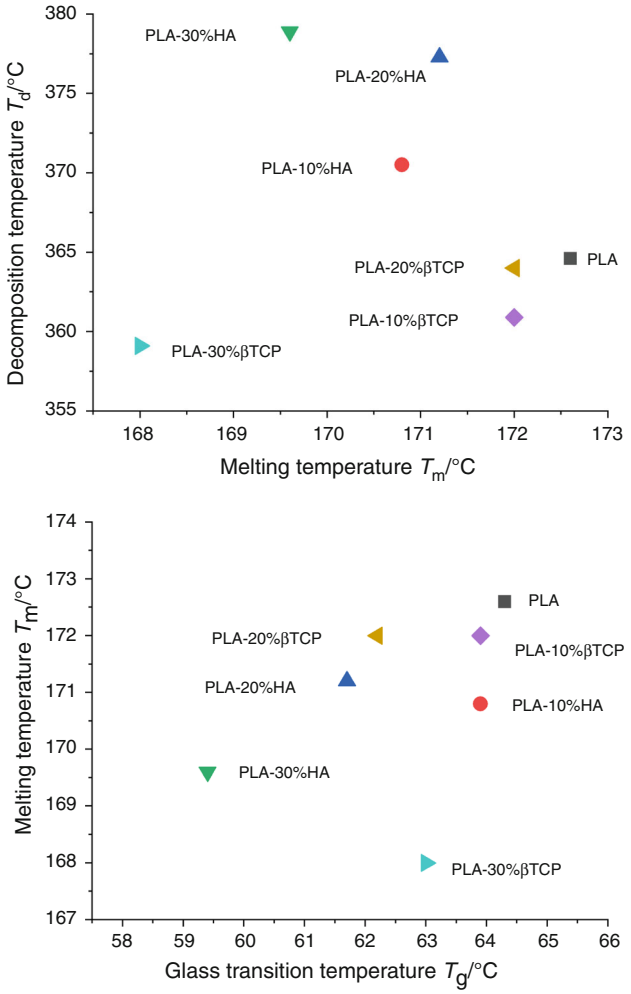

Fig. 10 Glass transition, melting and decomposition temperatures of unconditioned neat PLA, PLA/HA and PLA/βTCP composites

Conclusions

The main topic of this work is the in vitro conditioning of biodegradable composites formed by PLA matrix with different mass% HA and βTCP constitutive to determine the relevance of immersion time and fillers loading upon the thermal expansivity and thermal stability behaviour of these composites. It was found that both composite combinations show similar trends in their CTLE and thermal strain evolution with temperature, while the increase in the filler content gives rise to a decrease in the measured CTLE coefficients, inherent behaviour for these materials. More pronounced effects were registered with the βTCP filler, irrespective of the mass% content, giving rise to an enhanced thermal stability. Further, immersion time increase leads to an increasing tendency of CTLE values in all composites that can be regarded to the dissolution of HA and βTCP from the surface leaving the PLA constitutive to act as the main "contributor" to the property investigated. Certainly, manufacturing process itself and processing conditions may pose an influence on the results, but further investigations were not tackled in this study.

Concerning the thermogravimetric measurements, all in vitro conditioned PLA-based composite samples follow a single-step decomposition process, with differences due to the filler type and content. Among all, the PLA/HA combinations revealed enhanced onset temperatures on their decomposition curves, highest mass change and relatively lowest value on the residues comparatively with their PLA/βTCP counterparts. The same apply with respect to the decomposition temperatures associated with the maximum peak of DTG curves.

Dynamic mechanical analysis on unconditioned PLA and PLA-based composites was added to provide insights in the glass temperatures, T_g, from the peak values in the tan δ curves. Sharp and higher peaks were found in the PLA/βTCP composites with direct consequences on their enhanced capacity to absorb mechanical energy and thus to

withstand frequency depended mechanical loadings. Further data processing under decomposition over melting and melting over glass transition temperatures facilitates improved comprehension on these PLA and PLA-based composites as well as comparison with other reported data from the literature.

The main conclusion that can be withdrawn from the present study is that the increase in HA or βTCP fillers content within the PLA matrix does not limit the composites material performance, even though in vitro conditioned for an extended time range. Moreover, the double-step manufacturing process, extrusion followed by injection moulding, is a comfortable and easy route in developing PLA, PLA/HA and PLA/βTCP composites with enhanced dynamic mechanical and thermal properties. These findings help to further tailor high-loaded osteoconductive fillers-reinforced PLA composites for various medical and engineering applications.

References

1. Auras R, Lim LT, Selke S, Tsuji H. Poly(lactic acid): structures, production, synthesis, and applications. New York: Wiley; 2010.
2. Murariu M, Dubois P. PLA composites: from production to properties. Adv Drug Deliv Rev. 2016;107:17–46.
3. Haaparanta A-M, Haimi S, Ellä V, Hopper N, Miettinen S, Suuronen R, et al. Porous polylactide/β-tricalcium phosphate composite scaffolds for tissue engineering applications. J Tissue Eng Regen Med. 2010;4(5):366–73.
4. Ahmed J, Varshney SK. Polylactides—chemistry, properties and green packaging technology: a review. Int J Food Prop. 2011;14(1):37–58.
5. Garlotta D. A literature review of poly(lactic acid). J Polym Environ. 2001;9(2):63–84.
6. Slomkowski S, Penczek S, Duda A. Polylactides—an overview. Polym Adv Technol. 2014;25(5):436–47.
7. Avinc O, Khoddami A. Overview of poly(lactic acid) (PLA) fibre. Fibre Chem. 2009;41(6):391–401.
8. Akindoyo JO, Beg MDH, Ghazali S, Heim HP, Feldmann M. Impact modified PLA-hydroxyapatite composites—thermo-mechanical properties. Compos A Appl Sci Manuf. 2018;107:326–33.
9. Nazhat SN, Kellomäki M, Törmälä P, Tanner KE, Bonfield W. Dynamic mechanical characterization of biodegradable composites of hydroxyapatite and polylactides. J Biomed Mater Res. 2001;58(4):335–43.
10. Ignjatovic N, Uskokovic D. Synthesis and application of hydroxyapatite/polylactide composite biomaterial. Appl Surf Sci. 2004;238(1):314–9.
11. Li J, Zheng W, Li L, Zheng Y, Lou X. Thermal degradation kinetics of g-HA/PLA composite. Thermochim Acta. 2009;493(1):90–5.
12. Zhang SM, Liu J, Zhou W, Cheng L, Guo XD. Interfacial fabrication and property of hydroxyapatite/polylactide resorbable bone fixation composites. Curr Appl Phys. 2005;5(5):516–8.
13. Akindoyo JO, Beg MDH, Ghazali S, Heim HP, Feldmann M. Effects of surface modification on dispersion, mechanical, thermal and dynamic mechanical properties of injection molded PLA-hydroxyapatite composites. Compos A Appl Sci Manuf. 2017;103:96–105.
14. Kang Y, Yao Y, Yin G, Huang Z, Liao X, Xu X, et al. A study on the in vitro degradation properties of poly(l-lactic acid)/β-tricalcuim phosphate(PLLA/β-TCP) scaffold under dynamic loading. Med Eng Phys. 2009;31(5):589–94.
15. Huang J, Ten E, Liu G, Finzen M, Yu W, Lee JS, et al. Biocomposites of pHEMA with HA/β-TCP (60/40) for bone tissue engineering: swelling, hydrolytic degradation, and in vitro behavior. Polymer. 2013;54(3):1197–207.
16. Bleach NC, Nazhat SN, Tanner KE, Kellomäki M, Törmälä P. Effect of filler content on mechanical and dynamic mechanical properties of particulate biphasic calcium phosphate—polylactide composites. Biomaterials. 2002;23(7):1579–85.
17. Ferri J, Gisbert I, García-Sanoguera D, Reig M, Balart R. The effect of beta-tricalcium phosphate on mechanical and thermal performances of poly(lactic acid). J Compos Mater. 2016;50(30):4189–98.
18. Li X, Qi C, Han L, Chu C, Bai J, Guo C, et al. Influence of dynamic compressive loading on the in vitro degradation behavior of pure PLA and Mg/PLA composite. Acta Biomater. 2017;64:269–78.
19. Agrawal CM, McKinney JS, Lanctot D, Athanasiou KA. Effects of fluid flow on the in vitro degradation kinetics of biodegradable scaffolds for tissue engineering. Biomaterials. 2000;21(23):2443–52.
20. Kikuchi M, Koyama Y, Takakuda K, Miyairi H, Shirahama N, Tanaka J. In vitro change in mechanical strength of β-tricalcium phosphate/copolymerized poly-L-lactide composites and their application for guided bone regeneration. J Biomed Mater Res. 2002;62(2):265–72.
21. Lim LT, Auras R, Rubino M. Processing technologies for poly(lactic acid). Prog Polym Sci. 2008;33(8):820–52.
22. Ignjatovic N, Suljovrujic E, Budinski-Simendic J, Krakovsky I, Uskokovic D. Evaluation of hot-pressed hydroxyapatite/poly-L-lactide composite biomaterial characteristics. J Biomed Mater Res B Appl Biomater. 2004;71B(2):284–94.
23. Martin C. Twin screw extrusion for pharmaceutical processes. In: Repka MA, Langley N, DiNunzio J, editors. Melt extrusion: materials, technology and drug product design. New York: Springer; 2013. p. 47–79.
24. Cox SC, Thornby JA, Gibbons GJ, Williams MA, Mallick KK. 3D printing of porous hydroxyapatite scaffolds intended for use in bone tissue engineering applications. Mater Sci Eng C. 2015;47:237–47.
25. Corcione C, Scalera F, Gervaso F, Montagna F, Sannino A, Maffezzoli A. One-step solvent-free process for the fabrication of high loaded PLA/HA composite filament for 3D printing. J Therm Anal Calorim. 2018;134:1–8.
26. Siqueira L, Passador FR, Costa MM, Lobo AO, Sousa E. Influence of the addition of β-TCP on the morphology, thermal properties and cell viability of poly (lactic acid) fibers obtained by electrospinning. Mater Sci Eng C. 2015;52:135–43.
27. Drummer D, Cifuentes-Cuéllar S, Rietzel D. Suitability of PLA/TCP for fused deposition modeling. Rapid Prototyp J. 2012;18(6):500–7.
28. Ferri J, Jordá J, Montanes N, Fenollar O, Balart R. Manufacturing and characterization of poly(lactic acid) composites with hydroxyapatite. J Thermoplast Compos Mater. 2018;31(7):865–81.
29. Ferri J, Jordá J, Montanes N, Fenollar O, Balart R. Manufacturing and characterization of poly(lactic acid) composites with hydroxyapatite. J Thermoplast Compos Mater. 2018;31(7):865–81.
30. Menczel JD, Prime RB. Thermal analysis of polymers: fundamentals and applications. New York: Wiley; 2014.

31. Aboudi J, Arnold SM, Bednarcyk BA. Chapter 3—fundamentals of the mechanics of multiphase materials. In: Aboudi J, Arnold SM, Bednarcyk BA, editors. Micromechanics of composite materials. Oxford: Butterworth-Heinemann; 2013. p. 87–145.
32. Esposito Corcione C, Gervaso F, Scalera F, Padmanabhan SK, Madaghiele M, Montagna F, et al. Highly loaded hydroxyapatite microsphere/PLA porous scaffolds obtained by fused deposition modelling. Ceram Int. 2018;45:2803–10.
33. Zou H, Yi C, Wang L, Liu H, Xu W. Thermal degradation of poly(lactic acid) measured by thermogravimetry coupled to Fourier transform infrared spectroscopy. J Therm Anal Calorim. 2009;97(3):929.
34. Schindler A, Doedt M, Gezgin Ş, Menzel J, Schmölzer S. Identification of polymers by means of DSC, TG, STA and computer-assisted database search. J Therm Anal Calorim. 2017;129(2):833–42.
35. Lee WA, Knight GJ. Ratio of the glass transition temperature to the melting point in polymers. Br Polym J. 1970;2(1):73–80.